Developing a proof-of-concept process model for the techno-economic assessment of a modular geothermal Multi-Effect Distillation desalination plan

Neale Young, John Gilliland, Ken Maturgo, Duncan Steven

JRG Energy Consultants Ltd, PO Box 42246, Auckland 1745, New Zealand

Neale@jrgenergy.com

ABSTRACT

Freshwater scarcity affects millions, with projections indicating that by 2030, 700 million people may face displacement due to severe water shortage. In response, JRG Energy Consultants Ltd (JRG) have developed "Magnuvis", a geothermal desalination concept utilising an Organic Rankine Cycle (ORC) and Multi-Effect Distillation (MED) process. While previous feasibility assessments have informed its development, JRG seeks to refine the concept by creating an independent model for validation and optimisation.

This study presents a Geothermal ORC-MED Desalination model based on thermodynamic energy-mass balance analysis to assess its techno-economic viability. Initial results indicate that increasing geothermal resource mass flow rate enhances ORC network output and distilled water production and is consistent with expectations. Specifically, water production rates improve from 64 m³/day to 130 m³/day and 191 m³/day as brine flow rate rises from 30 kg/s to 60 kg/s to 90 kg/s respectively at a supply temp of 120°C. These results reflect similar trends observed in other studied works and show that this model serves as a foundation for system improvements and real-world deployment.

Keywords: Desalination, Geothermal, Multi-Effect Distillation, Organic Rankine Cycle.

1. INTRODUCTION

According to UNICEF, the most recent data on global water scarcity reveals that approximately four billion people – nearly two-thirds of the global population – experience severe water scarcity for at least one month each year. Water scarcity not only impairs access to safe drinking water but also has far-reaching implications for agriculture, industry, and economic development, ultimately threatening livelihoods and food security. Projections suggest that, by 2030, as many as 700 million people could be displaced due to acute water scarcity. As is often the case with environmental stressors, the impacts fall disproportionately on the poorest communities, many of which reside in rural, arid, and hard-to-reach regions where access to essential utilities such as affordable and reliable energy is also limited.

As shown in Figure 1, water stress and scarcity are predominantly concentrated in arid and semi-arid regions, particularly across the Middle East and North Africa (MENA), South, Central, and East Asia, parts of South America, and central-western North America as indicated with yellow to red scale – red indicating areas of increased water stress. These regions often rely on finite groundwater sources and face challenges in securing sustainable freshwater supplies.

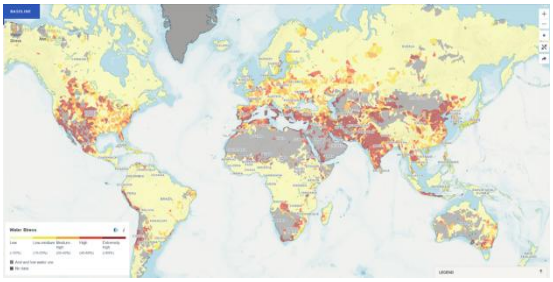


Figure 1: Global water stress map.

Although approximately 71% of the Earth's surface is covered by water, around 96.5% of it is saline or brackish, rendering it unfit for human consumption. Of the remaining, only 2.5% is considered freshwater with approximately 68.7% of that locked in glaciers and permanent snow cover, primarily in polar regions. This leaves only about 0.26% of the Earth's total water readily accessible and safe for human use (Gleick et al., 1993). Given this stark disparity between the abundance of saline water and the scarcity of potable freshwater, desalination presents itself as an increasingly vital solution: the process of converting seawater or brackish water into freshwater suitable for human and industrial use.

It is for this very reason that the Magnuvis concept – an IP holding of JRG Energy Consultants Ltd. – was developed. It's modular, containerised design is such that it can be transported and deployed independently, allowing flexible configuration to suit specific site constraints (Figure 2).

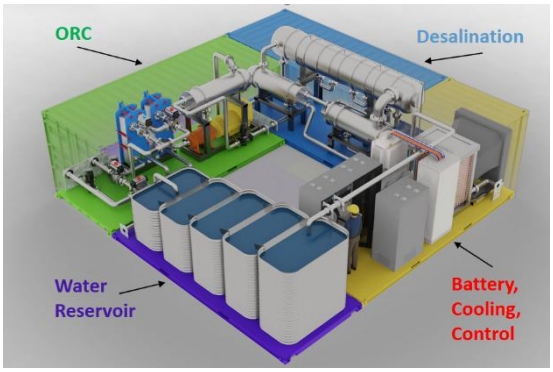


Figure 2: Modularised concept ORC-MED plant "Magnuvis"

While detailed mechanical specifications, such as heat exchanger sizing and MED stage configuration, are beyond the scope of this paper, energy and mass balance modelling will be the focus to enable a first pass at a techno-economic feasibility and viability assessment across varying geothermal conditions. The results of which will support early-stage optimization and provide a foundation for future pilot-scale implementation.

2. METHODOLOGY/APPROACH

2.1 MULTI-EFFECT DISTILLATION (MED) TECHNOLOGY

Multi-Effect Distillation (MED) is a widely adopted thermal desalination technology, particularly suited for seawater treatment. In addition to its desalination applications, MED is also used across several industrial processes including sugar refining, dairy production, paper and pulp processing, and chemical manufacturing (Catrini et al., 2018). In desalination, the primary product is purified distillate, while in industrial settings the focus may be on the concentrated output.

The MED process involves a series of sequential stages, or "effects," typically ranging from 3 to 16 depending on plant size and energy input. Each effect operates at progressively lower pressures and temperatures, enabling water to evaporate at reducing boiling temperatures. Vapour produced in one effect condenses in the next, transferring latent heat to incoming feedwater maximizing system efficiency. This cascading mechanism allows for significant energy recovery and results in lower specific thermal energy consumption (STEC) compared to other thermal methods (Catrini et al., 2018).

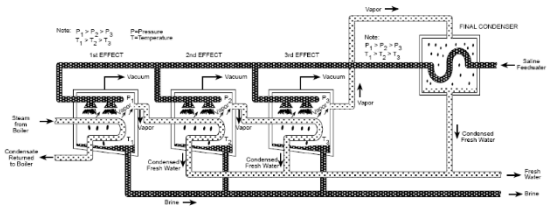


Figure 3: PF-MED process used for the modelling of the techno-economic assessment (National research Council, 2008).

2.2 ORGANIC RANKINE CYCLE (ORC) TECHNOLOGY

The Organic Rankine Cycle (ORC) is a mature and increasingly adopted technology in the geothermal power sector, particularly advantageous for utilizing low to medium-enthalpy geothermal resources. Unlike conventional steam Rankine cycles, ORCs

employ organic fluids with lower boiling points, enabling efficient energy conversion from resources with temperatures ranging from below 100°C to as high as 300°C as a standard inlet temperature, with latest developments for biomass application operating at 400°C with efficiencies greater than 30% (National research Council, 2008). When integrated with MED, ORCs can enable a fully self-sustaining desalination systems in off-grid or remote locations.

The ORC process follows a similar thermodynamic sequence to the traditional Rankine cycle and is shown below in **Error! Reference source not found.**Figure 4 where the organic working fluid is vaporized by geothermal brine in the evaporator (3 to 6), expanded through a turbine or expander to generate electricity (6 to 7), passed through a recuperator to recover residual heat (7 to 8), and then condensed (8 to 1) before being recirculated via a feed pump (1 to 2) and again passing through the other side of the recuperator (2 to 3) before stating the cycle again. In the proposed system, the condenser stage of the ORC is thermally coupled with the first effect of the MED unit.

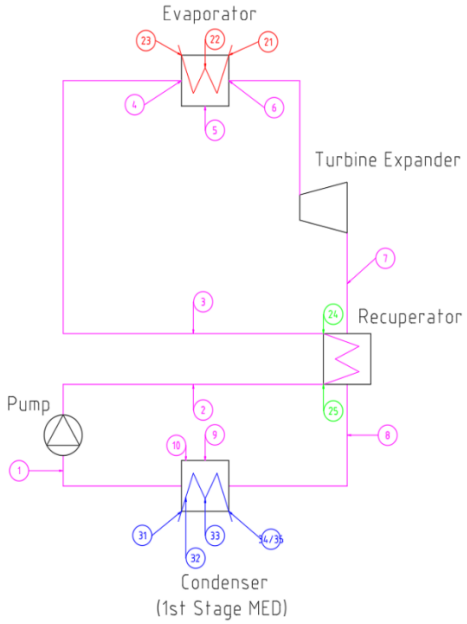


Figure 4. Process Flow Diagram for the ORC System.

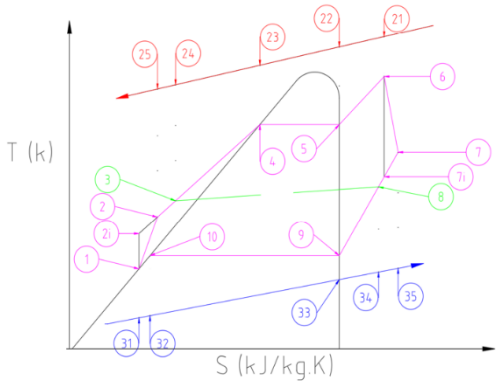


Figure 5. T-S diagram for the respective ORC system.

The initial step in developing the ORC thermodynamic model involved interpreting the temperature–entropy (T–S) diagram (refer to Figure 4.B**Error! Reference source not found.**) to define the characteristic states of the working fluid throughout the cycle. For this analysis, it is assumed that the working fluid experiences mild superheating in the evaporator and slight subcooling in the condenser. While the extent of superheat and subcooling is highly dependent on the specific working fluid and its compatibility with the geothermal heat source, this study applied standardised values of +5 °C superheat and −5 °C subcooling for consistency. Determining the optimal working fluid and associated thermal characteristics was outside the scope of this paper.

The heat source – geothermal brine in this case – was assumed to remain in the single-phase liquid state throughout the process, i.e., no phase change occurs. To simplify the modelling approach, a constant surface wellhead pressure of 10 bar was applied for all geothermal brine conditions. This pressure was selected as the minimum required to maintain a brine temperature of 180 °C in single-phase and was uniformly applied across all brine flow rates. The appropriateness of this assumption is also topic for discussion for further modelling and assessment.

The ORC system model was developed using Microsoft Excel with the CoolProp{Bell, 2024 #47} add-in,

enabling efficient lookup of thermophysical properties based on a minimum of two known state variables. The model architecture was validated against published sources focused on energy mass balance assessments in desalination processes (Catrini et al., 2018; Gude, 2016; Karagiannis & Soldatos, 2008; National research Council, 2008; Xu et al., 2024)

To initiate the ORC modelling, the system's operating temperature limits were first defined. The low-pressure boundary is constrained by the condenser, which doubles as the first stage of the MED unit, and is limited to a maximum temperature of 70 °C. This sets the corresponding saturation pressure, represented by the lower isobar on the T–S diagram (between points 10 and 9). The upper operating temperature, corresponding to the evaporator, was varied parametrically from >100 °C to 180 °C to evaluate system performance under different conditions. This defines the upper saturation line (between points 4 and 5 on the T–S diagram).

Once the temperature and pressure boundaries were established, a node-by-node thermodynamic analysis was carried out. Each state point (node) in the ORC system was solved sequentially using first-law energy and mass balance equations, supplemented by CoolProp property lookups where at least two independent thermodynamic properties (e.g., pressure, temperature, enthalpy, entropy, or vapour quality) were known. Table 1 is an example of how this nodal analysis was carried out and outlines the nodal approach used to determine the full thermodynamic state of the working fluid throughout the ORC loop.

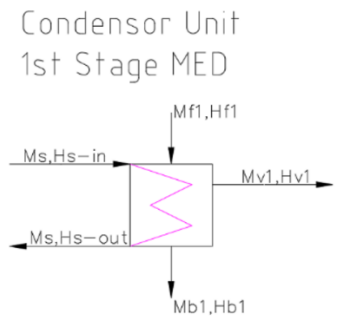
Table 1: Nodal analysis results for the working fluid in the ORC.

Node	Knowns	Calculated	CoolProp Look-up
4	T = 90°C P = 0.54 bar (Sat' P, 90°C) Quality = 0	N/A	H, S
5	T = 90°C P = 0.54 Bar (Sat' P, 90°C) Quality = 1	N/A	P, H, S
9	T = 70°C P = 0.27 Bar (Sat' P, 70°C) Quality = 1	N/A	P, H, S
10	T = 70°C P = 0.27 Bar (Sat' P, 70°C) Quality = 0	N/A	P, H, S
1	T = 65°C (sub-cooled) P = 0.27bar, P at node (10)	N/A	H, S, X
2i	P = 0.54 bar, P at node (4, 5) S = S at node (1), isentropic compression	N/A	T, H, X
2	P = 0.54 bar, P at node (4, 5)	H, calculated between nodes 1 & 2i using pump efficiency.	T,S, X
3	P = 0.54 bar, P at node (4, 5)	H, calculated from H (node 2), Q rejected from system and mass flow rate.	T, S, Z
6	P = 0.54 bar, P at node (4, 5) T= 95°C (Superheated)	N/A	H, S, X
7i	P = 0.27 bar, P at node (9, 10) S = S at node (6), isentropic expansion)	N/A	T, H, X
7	P = 0.27 bar, P at node (9, 10)	Enthalpy calculated between nodes 6 & 7i using expander efficiency.	T, S, X
8	P = 0.27 bar, P at node (9, 10) T = T at node (2) + ΔT_{pp} = 75°C	N/A	T, S, X

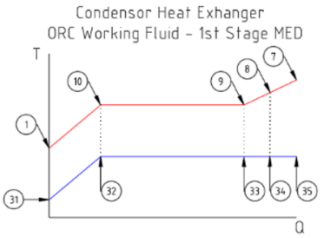
A similar nodal analysis was also applied to the evaporator and condenser units to complete the ORC unit analysis. Once this was full described the inlet parameters for the MED unit can then be applied to the nodal analysis of the MED system and systematic solved for each effect.

2.3 MULTI-EFFECT DISTILLATION MODELLING AND NODAL ANALYSIS

As earlier described, the condenser has been designed as first stage of the MED. As with the ORC a free body diagram of the process flow is the best place to start with accompanying T-Q diagrams before going on to complete the nodal analysis of the MED system and is shown in Figures 6-8.

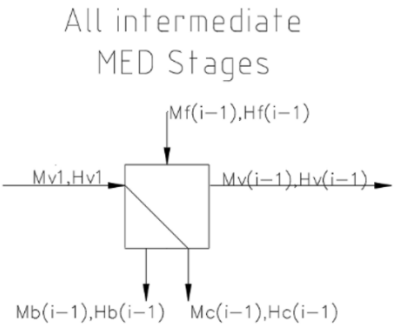


(A)

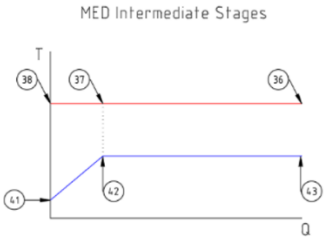


(D)

Figure 6. PFD for Energy Mass Balance and Nodal analysis with respective T-Q Diagrams for condenser and 1st stage MED unit.

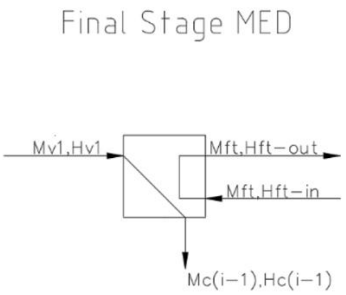


(B)

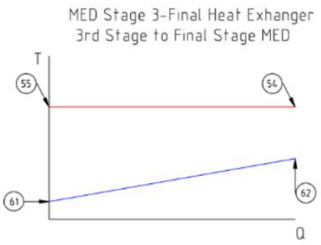


(E)

Figure 7. PFD for Energy Mass Balance and Nodal analysis with respective T-Q Diagrams for all intermediate stages.



(C)



(F)

Figure 8. PFD for Energy Mass Balance and Nodal analysis with respective T-Q Diagrams for final stage MED.

For this system configuration, a parallel-feed strategy is applied. That is, each effect receives independent feedwater introduced at the same initial temperature (either ambient or preheated) and is heated internally to the boiling temperature of the effect. In all stages, the condensing vapour enters as a saturated vapour and exits as a saturated liquid, transferring its latent heat to the feedwater side in each effect. The vapour-side nodes are modelled identically to a forward-feed configuration. However, the feedwater-side nodal structure is adapted to reflect the parallel nature of the flow.

With the nodal analysis completed for the condenser unit it is now possible to complete the energy mass balance calculation for mass flow rate of feedwater to the condenser unit / first stage MED as well as complete a solids mass balance to quantify the brine and vapour generated in the first Stage (effect). This process is then repeated for each effect until the system is fully described for a given input of geothermal brine flow rate and temperature.

3. RESULTS AND DISCUSSIONS

3.1 ORC RESULTS

Figure 6 presents the temperature–entropy (T–S) diagram for an Organic Rankine Cycle (ORC) system utilizing toluene as the working fluid, with a condenser temperature of 70 °C and an evaporator temperature of 90 °C. The cycle includes 5 °C of superheat and 5 °C of subcooling. The system was analysed over a geothermal brine input temperature range of 101 °C to 180 °C, with state points plotted against the saturation curve for toluene. The modelled cycle closely aligns with the expected thermodynamic path, indicating good agreement with the toluene saturation properties and validating the model's thermodynamic fidelity. While the selected operating limits are reasonable, they should be fine-tuned for specific applications; however, such optimization lies outside the scope of this study.

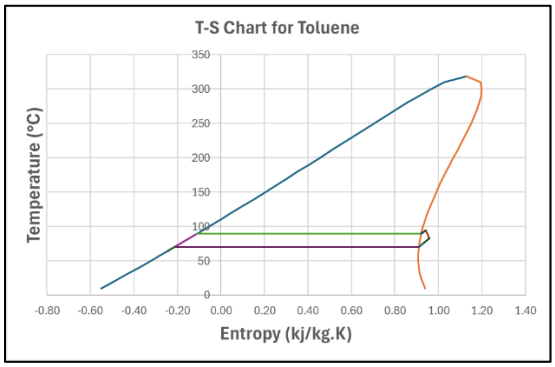


Figure 9. T-S diagram for an ORC system with Toluene as a working fluid

Figure 7 illustrates the corresponding heat input and work output profiles. These energy flows follow a pattern similar to the efficiency trend, as both are fundamentally governed by the thermodynamic properties of the working fluid. The strong correlation further supports the internal consistency and robustness of the ORC model.

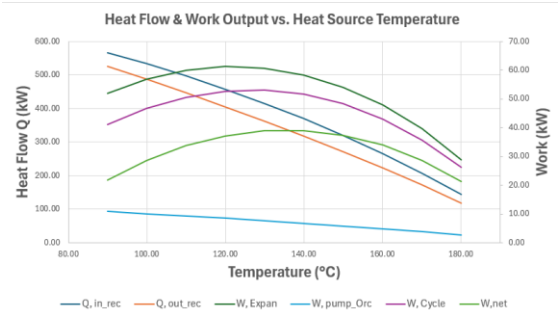


Figure 10. Cycle heat and work energy flows vs. Geothermal Brine Feed Temperature.

In summary, the simulation results are consistent with theoretical expectations and provide confidence in the reliability and accuracy of the ORC subsystem model.

3.2 MED SYSTEM RESULTS

Following the successful validation of the ORC subsystem, the coupled MED-ORC model was evaluated to assess overall distillate production and net power output. Simulations were performed across three geothermal brine flow rates - 30 kg/s, 60 kg/s, and 90 kg/s – and a range of inlet temperatures from 101 °C to 180 °C. The resulting outputs, namely net electrical power and distillate yield were monetised using representative regional pricing data for Chile (a local area). These economic indicators are presented in Figure 8 as a bubble chart, where bubble size reflects total system revenue.

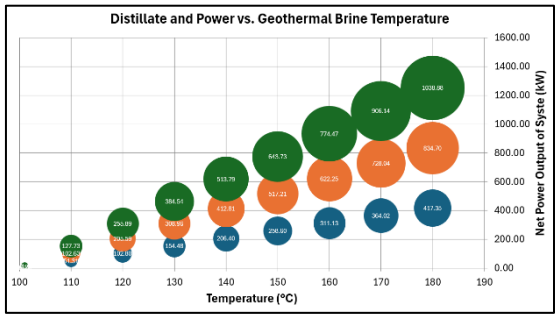


Figure 11. Bubble chart showing system revenue for increasing geothermal brine feed temperature.

Encouragingly, the model developed in this study demonstrates both qualitative and quantitative alignment with the findings of Birney et al. (Birney et al.,

2019), with overall trends and output magnitudes showing close agreement. The similarity in performance metrics enhances confidence in the validity of the MED model as well as its integration within the larger hybrid system.

A noted discrepancy in output values is attributed primarily to differences in plant configuration. Specifically, Birney et al. incorporated an Electric Submersible Pump (ESP) to assist geothermal fluid extraction, whereas this model assumes unassisted well flow. The implications of this design choice, along with other plant-level assumptions, are topic for future discussion and system refinement.

3.3 ECONOMIC ANALYSIS

Due to the scope limitations of the thermodynamic model, equipment sizing and component-level cost estimates are not directly available. Consequently, a detailed capital cost breakdown for each plant subsystem is beyond the intention of this study. However, by leveraging the energy and mass balance outputs for net electrical power and distilled water production, a first-pass economic assessment was performed to evaluate the conceptual viability of the integrated ORC-MED system.

The revenue model for the system was based on surplus energy and freshwater production and covered three scenarios:

1. Scenario A: 30 kg/s flow at 110 °C (Low)
2. Scenario B: 60 kg/s flow at 140 °C (Mid)
3. Scenario C: 90 kg/s flow at 170 °C (High)

Below is a tabulated summary of results for the thress scenarios. The results of which were used in subsequent discounted cash-flow analysis showing expected payback periods.

Table 2: Summary of scenario results used for economic simulation.

Parameter	Units	Scenario A	Scenario B	Scenario C
ORC Net Power Output	kW	51.13	324.68	1,089.28
ORC CAPEX	US$	127,958.37	1,029,382.38	2,723,194.25
ORC OPEX (2%)	US$	2,559.17	20,587.65	54,463.89
MED Output	m^3/day	42.58	330.85	874.77
MED CAPEX	US$	261,348.98	1,318,838.87	3,305,904.78
MED OPEX	US$	29,280.39	172,853.43	442,632.93
Well CAPEX	US$	234,865.02	1,889,291.30	5,011,417.45
Annual ORC Revenue	US$	52,592.44	423,088.59	1,119,265.72
Annual MED Revenue	US$	17,375.95	139,783.70	369,792.79
ORC Net Power Output	kW	51.13	324.68	1,089.28

Not that the intention here is to demonstrate financial viability at a conceptual level and not guarantee cash return from the modelled systems i.e. they support a 'Go-No/Go' analysis on further development of the concept.

3.3.1 Scenario A



Figure 9. Discounted payback period for Scenario A: Low flow rate (30 kg/s) / Low geothermal brine temp (110°C).

3.3.2 Scenario B



Figure 10. Discounted payback period for Scenario B: Medium flow rate (60 kg/s) / Mid geothermal brine temp (140°C).

3.3.3 Scenario C



Figure 11. Discounted payback period for Scenario C: High flow rate (90 kg/s) / High geothermal brine temp (170°C).

4. SUMMARY AND CONCLUSIONS

The integrated ORC-MED model developed in this study successfully accepts a wide range of input parameters and provides a comprehensive set of output variables, including thermodynamic performance, distillate yield and net power production. These outputs have been benchmarked against established literature, notably the work of Birney et al., with encouraging alignment, thereby validating both the technical and conceptual integrity of the model.

A simple economic analysis was also run to sense check the viability of the concept. Results indicate that more work would be required prior to any final investment decision into a potential pilot plant though are sufficient to indicate further refinement and development of the model should be undertaken and strongly indicate that further viability could be more robustly proven supporting future investment decision in to a pilot plant with refinement of the model.

REFERENCES

Birney, C. I., Jones, M. C., & Webber, M. E. (2019). A Spatially Resolved Thermodynamic Assessment of Geothermal Powered Multi-Effect Brackish Water Distillation in Texas. *Resources*, *8*(2), 65. https://www.mdpi.com/2079-9276/8/2/65

Catrini, P., Cipollina, A., Giacalone, F., Micale, G., Piacentino, A., & Tamburini, A. (2018). Chapter 12 - Thermodynamic, Exergy, and Thermoeconomic analysis of Multiple Effect Distillation Processes. In V. G. Gude (Ed.), *Renewable Energy Powered Desalination Handbook* (pp. 445-489). Butterworth-Heinemann. https://doi.org/https://doi.org/10.1016/B978-0-12-815244-7.00012-X

Gleick, P., White, G. F., Pacific Institute for Studies in Development, E., Security, & Stockholm Environment, I. (1993). *Water in crisis : a guide to the world's fresh water resources*. Oxford University Press.

Gude, V. G. (2016). Geothermal source potential for water desalination – Current status and future perspective. *Renewable and Sustainable Energy Reviews*, *57*, 1038-1065. https://doi.org/https://doi.org/10.1016/j.rser.2015.12.186

Karagiannis, I. C., & Soldatos, P. G. (2008). Water desalination cost literature: review and assessment. *Desalination*, *223*(1), 448-456. https://doi.org/https://doi.org/10.1016/j.desal.2007.02.071

National research Council. (2008). *Desalination - A National Perspective* (Vol. 1). The National Acadamies PRess. https://nap.nationalacademies.org/read/12184/chapter/1

Xu, B., Yang, X., Zhou, J., Guo, P., Yao, X., Ma, L., Jiao, H., Tian, B., & Zhang, X. (2024). Renewable energy-driven for sustainable off-grid desalination: A comprehensive review on technical highlights and process. *Desalination and Water Treatment*, *320*, 100803. https://doi.org/https://doi.org/10.1016/j.dwt.2024.100803